Neuroradiology (1993) 35: 113–118

Neuro radiology

Posterior cranial fossa dimensions in the Chiari I malformation: relation to pathogenesis and clinical presentation

L. J. Stovner[1], U. Bergan[2], G. Nilsen[3], and O. Sjaastad[1]

Departments of [1] Neurology and [2] Radiology, Trondheim University Hospital, and [3] MR-Centre, University of Trondheim, Trondheim, Norway

Received: 7 April 1992

Summary. Skull dimensions were measured on lateral skull radiographs in 33 adult patients with MRI-verified Chiari I malformations and in 40 controls. The posterior cranial fossa was significantly smaller and shallower in patients than in controls. In the patients, there was a positive correlation between posterior fossa size and the degree of the cerebellar ectopia, which might indicate that a posterior cranial fossa which was originally too small had been expanded by the herniation of hindbrain structures at an early stage. Pyramidal signs and cerebellar symptoms and signs, which may be due to compression of neural structures, were associated with a large degree of ectopia and a relatively large posterior cranial fossa. Syringomyelia and headache, which may be due to the valve action of the herniated cerebellar tissue, were not associated with a particularly large posterior fossa or herniation. No special clinical presentation was associated with a very small posterior cranial fossa, which may indicate that a small posterior cranial fossa per se has little or no clinical significance, although it may be the primary developmental anomaly.

Key words: Chiari I malformation – Magnetic resonance imaging – Pathogenesis – Posterior cranial fossa – Skull radiography

In patients with the Chiari I malformation (CM-1), there is caudal displacement of the cerebellar tonsils and sometimes part of the medulla oblongata [1, 2]. This condition may be associated with a small, shallow posterior cranial fossa (PF), as well as other malformations of the base of the skull and cervical spine such as occipitalization of the atlas, fusion of cervical vertebrae, spina bifida, basilar impression, and platybasia [3–6]. It has been suggested that the bony malformations, and notably a small PF, are fundamental in this condition, and that the neural malformations are secondary [6–8].

Magnetic resonance imaging (MRI) enables precise measurement of the extent of the herniation and rather certain diagnosis of syringomyelia. The aim of the present study was to investigate quantitatively the relationship between these aspects of the malformation and the size and shape of the skull, particularly the PF. We also wished to clarify whether abnormal skull dimensions might be associated with particular clinical presentations. We hoped that this might shed some light on the pathogenesis of the malformation itself and of the different clinical presentations.

We tried to assess the value of Krogness's method for skull mensuration [9] by comparing the results obtained with those obtained by previously used methods, and to assess the value of the method as a screening test for the malformation, as has been suggested [10].

Methods

Patients

Thirty-three patients (11 men, 22 women; mean age 50 years, range: 24–67 years) with CM-1 were studied. They had not been subjected to PF decompression, and they consented to have a skull radiograph for this study. Clinical data are given in Table 1. One was totally asymptomatic. In some of the others, there may be doubt as to whether the symptoms and signs were caused by the malformation; for example, 2 patients had progressive muscle atrophy which may be due to the malformation [11], but which was probably due to motor neuron disease. Thirteen patients had only subjective symptoms such as pain or intermittent dizziness or unsteadiness, with no neurological deficit or signs of syringomyelia on MRI. These symptoms are nonspecific, but probably due to the malformation in the majority. In the remaining 18 patients (later referred to as the group with "definite pathology" due to the malformation), clear neurological signs or syringomyelia, demonstrated by MRI, were attributable to the malformation.

Controls

A control group of skull radiographs (40 adults, age > 17 years) was selected from the radiology files. The films had been taken for various reasons, mostly accidents, but showed no evidence of trauma. The control group was sex-matched with the groups of patients; otherwise it was selected on a random basis.

Table 1. Clinical features and MRI findings

Case	Sex	Age (years)	Extent of		Posterior fossa (PF) ratio	Clinical data
			cerebellar ectopia (mm)	syringomyelia (segments)		
1	M	53	5		12.4	Head and arm pain
2	M	46	10	C1–T4	13.8	Cerebellar signs
3	F	64	7		13.9	Head and neck pain
4	F	67	8		14.0	Headache
5	M	24	10		14.2	Asymptomatic
6	F	62	8		14.2	Trunk pain, sensory loss
7	M	48	6		14.4	Intracranial hypertension
8	M	34	14	C1–C6	14.6	central cord syndrome
9	F	36	5		14.7	Headache
10	F	55	5		14.7	Brain-stem involvement
11	F	37	6		14.7	Cerebellar symptoms, headache
12	M	62	5		14.9	Cerebellar symptoms
13	M	56	20		15.0	Cerebellar and pyramidal signs
14	M	32	9		15.0	Headache, syncopal attacks
15	F	59	12		15.0	Neck and arm pain
16	M	50	10		15.4	Muscle atrophy
17	F	67	15		15.4	Headache, trunk sensory loss
18	F	36	6		15.5	Headache
19	F	62	9	C1–T10	15.5	central cord syndrome
20	F	51	15		15.7	Cerebellar signs
21	F	54	12	Medulla–L2	16.0	central cord syndrome
22	F	66	20		16.1	Cerebellar symptoms, pyramidal signs
23	F	63	10	C1–T12	16.4	Head and arm pain, sensory loss, cerebellar signs
24	F	46	12	C6–T4	16.8	Head, neck and arm pain
25	F	54	14		16.9	Head and neck pain
26	F	43	15		17.0	Cerebellar symptoms
27	F	36	5		18.0	Headache and neck pain
28	F	66	18	C1–C6	18.4	Headache, cerebellar symptoms
29	F	41	30		18.7	Headache, pyramidal signs, cerebellar symptoms
30	F	39	22		18.9	Cerebellar and pyramidal signs
31	F	29	10	C1–C7	19.0	Cerebellar and pyramidal signs
32	M	59	12		19.2	Muscle atrophy
33	M	48	21		21.0	Cerebellar and brain-stem signs

Magnetic resonance imaging

All patients were examined with a 0.5T or a 1.5T whole body MRI system. The extent of cerebellar tissue ectopia was measured in the midsagittal plane on T1-weighted images of the brain or brain stem. The lower border of the foramen magnum was represented by a line from the lowest point of cortical bone (seen by a lack of signal) at the basion to the lowest point at the opisthion, as suggested previously [12, 13]. The appearances were considered pathological when the lowest point of the cerebellar tonsils lay ≥ 5 mm below this line [13]. In addition to cerebellar ectopia, slight enlargement of one or more ventricles was found in 3 patients, and syringomyelia in 8. None had (myelo)meningocele, or other malformations.

Plain radiographs

The films were interpreted in a blinded manner by the radiologist (U.B.).

Measurements were made on the lateral radiographs, as described by Krogness [9] (Fig. 1). The nasion (N), tuberculum sellae (Ts) and internal occipital protuberance (IOP) were used as reference points, the distance IOP-Ts representing Twinings line (Tw). Tw was divided into four equal segments. One perpendicular line was raised at a distance of $^1/_4$ Tw from Ts up to the inner table of the vertex (Tw-vertex), and another was drawn at a distance of $^1/_4$ Tw from the IOP up to the inner table of the skull (H) and down to the inner table of the PF (h).

Using Krogness's empirical formulae based on comparison with planimetric findings, the supratentorial area above Tw was calculated as ($^1/_2$ (N-Ts) + Tw) × (Tw-vertex), and the PF area below Tw as $^3/_4$ Tw × h. The ratios h/H, h/Tw and the PF ratio (PF area/supratentorial area × 100) were then calculated.

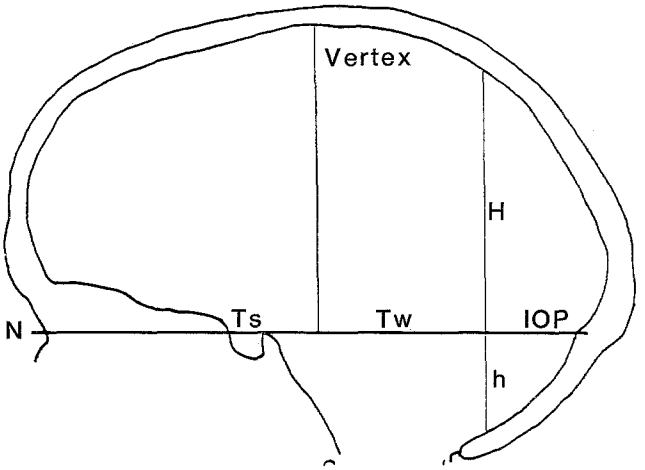

Fig. 1. Diagram of the midsaggittal plane of normal skull, showing the lines drawn for measurement. *IOP,* internal occipital protuberance; *N,* nasion; *Ts,* tuberculum sellae; *Tw,* Twining's line (between Ts and IOP) (Adapted with permission from [9])

Table 2. Ratios and measurements on skull radiographs

Variables	Women		*P*	Men		*P*
	Controls (26)	Patients (22)		Controls (14)	Patients (11)	
Tw (mm)	112.1 ± 8.8	110.2 ± 8.0	0.5	117.1 ± 6.0	117.8 ± 8.9	0.8
N-Ts (mm)	71.3 ± 6.3	68.1 ± 4.3	0.05	75.2 ± 5.6	76.6 ± 0.5	0.5
Tw-Vertex (mm)	110.5 ± 8.1	108.4 ± 5.4	0.3	118.4 ± 7.1	117.8 ± 7.0	0.8
H (mm)	96.1 ± 8.0	94.8 ± 6.7	0.5	102.0 ± 9.0	106.2 ± 8.5	0.2
h (mm)	33.2 ± 3.8	30.5 ± 2.8	0.008	36.9 ± 5.4	32.3 ± 5.2	0.04
Supratentorial area (cm^2)	163.9 ± 23.2	156.6 ± 15.0	0.2	182.5 ± 17.2	185.2 ± 20.6	0.7
PF area (cm^2)	28.0 ± 4.7	25.2 ± 2.6	0.02	32.4 ± 5.4	28.6 ± 5.5	0.1
h/H ratio (%)	34.7 ± 4.3	32.4 ± 4.2	0.07	36.4 ± 5.9	30.6 ± 5.7	0.02
h/Tw ratio (%)	29.7 ± 3.1	27.9 ± 3.6	0.07	31.5 ± 4.5	27.4 ± 4.1	0.03
PF ratio (%)	17.1 ± 1.7	16.2 ± 1.6	0.05	17.8 ± 2.7	15.4 ± 2.5	0.03

For abbreviations, see Methods section

Table 3. PF area estimated in three different studies

	PF area (cm^2) (mean ± SD)			
	Females		Males	
	Controls	CM-1	Controls	CM-1
Schady et al. [8]	31.4 ($n = 23$)	24.7 ($n = 19$)	35.5 ($n = 26$)	26.7 ($n = 13$)
Vega et al. [7]	25.7 ± 2.3 ($n = 23$)	22.0 ± 3.3 ($n = 17$)	27.9 ± 3.0 ($n = 23$)	22.0 ± 3.3 ($n = 25$)
Present study	28.0 ± 4.7 ($n = 26$)	25.2 ± 2.6 ($n = 22$)	32.4 ± 5.4 ($n = 14$)	28.6 ± 5.5 ($n = 11$)

Table 4. Ratios on skull radiographs

Ratio	Controls (40)	CM-1 (33)	*P*
h/H (%)	35.3 ± 4.9	31.8 ± 4.7	0.003
h/Tw (%)	30.3 ± 3.7	27.7 ± 3.7	0.004
PF ratio (%)	17.4 ± 2.1	15.9 ± 1.9	0.003

Statistical methods

The Student's *t*-test was used to search for possible differences between groups, and Pearson's *r* was calculated for possible correlations between variables. A two-tailed *P* value of less than 0.05 was considered statistically significant. To assess the value of PF measurement as a screening method, the positive and negative predictive values were calculated, using Bayes's theorem [14].

Results

The measurements on skull radiographs are given separately for men and women in Table 2. Patients of both sexes had significantly lower mean values for h than the corresponding control groups. Except for a somewhat lower mean value of N-Ts in female patients as compared to female controls, all other absolute measures (Tw, Tw-vertex, and H) were similar in patients and controls. The lower mean values in patients with regard to all the calculated PF variables (PF area, h/H ratio, h/Tw ratio, and PF ratio) are therefore most probably due to the difference in h. Among the ratios, the difference reached statistical significance for both sexes only with regard to the PF ratio.

In two previous studies on CM-1 patients and controls [7, 8], the PF area was by determined by planimetry on lateral radiographs. The mean values obtained with Krogness's method in the present study are similar to those obtained with planimetry (Table 3), but the differences between patients and controls are somewhat smaller in the present study.

The ratios for the whole patient group are shown in Table 4. Unlike the absolute measure h the ratios are not affected by variations in magnification on the film or by sex differences in absolute skull size. As a putative screening method for the CM-1, it might therefore seem reasonable to choose, for example, the PF ratio, instead of the absolute measure h, but there is considerable overlap between the two groups (Fig. 2). By trying systematically to discriminate with several cutoff values, we found the optimal value to be 15.8 %, which gave a sensitivity of 0.61 and a specificity of 0.80. The prevalence of the CM-1 in the general population is not known. If CM-1 were to occur in $^1/_{100}$ in the general population (possibly a too high esti-

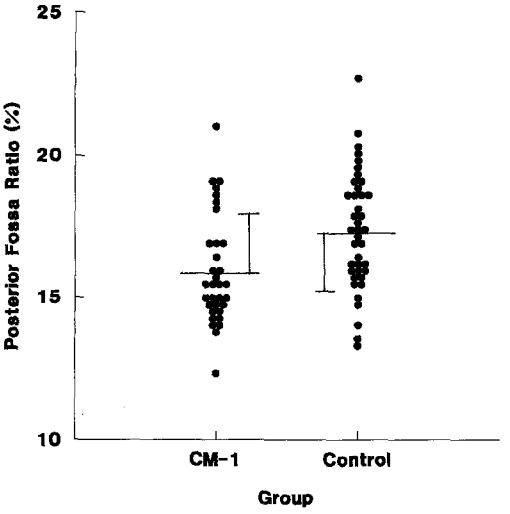

Fig. 2. Posterior fossa ratio (mean ± SD) in 33 patients with Chiari I malformation and 40 controls

Table 5. Correlation coefficients *(r)* of skull measurements and degree of cerebellar ectopia in 33 CM-1 patients

N-Ts	Tw	H	Supratentorial area	h	h/H	PF ratio	PF area
0.12	0.05	−0.17	−0.05	0.50**	0.52**	0.58***	0.41*

Two-tailed p values: * ≤0.05, ** ≤0.01, *** ≤0.001

mate), the positive predictive value of a PF ratio below cutoff would be only 0.030, and the negative predictive value of a PF ratio at cutoff or higher would be 0.995.

In the CM-1 group, statistically significant positive correlations were found between the extent of cerebellar ectopia and the PF variables (Table 5), especially with regard to the PF ratio ($r = 0.58, P \leq 0.001$) (Fig. 3).

In Table 6, the patients with and without definite clinical manifestations of the malformation are compared as to extent of cerebellar ectopia and PF ratio, as are patients with and without cerebellar involvement, pyramidal signs, syringomyelia or headache. As to the degree of cerebellar ectopia, very significantly larger values are found in those patients who have definite pathology due to the malformation, evidence of cerebellar involvement or pyramidal signs. In contrast, no significant differences were found if we compared those patients who had syringomyelia or headache with those who had not. Significantly larger PF ratios were found in patients who had pyramidal signs or evidence of cerebellar involvement than in those who had not. Only insignificant differences existed in the other clinical categories.

Discussion

In the present study, we have not tried to determine the volume of the PF. Such determination has been performed on CT scans by Vega et al. [7], who found that the PF volume was correlated with the PF area (controls: $r = 0.484$, patients: $r = 0.384$). The difference between patients and controls was, however, more significant with regard to the PF area ($P < 0.001$ both for males and females), the PF depth ($P < 0.005$ both for males and females) and the clivus length ($P < 0.001$ both for males and females) than with regard to the PF volume ($P < 0.05$ for males, not significant for females). This fact may indicate that the depth and shape of the PF as seen in the midsagittal section are better estimators of the fundamental PF abnormality in the CM-1 than the actual PF volume.

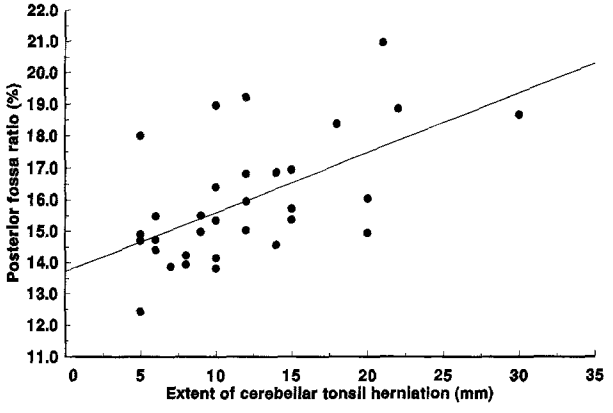

Fig. 3. Posterior fossa ratio plotted against degree of cerebellar ectopia. Linear regression equation: posterior fossa ratio (%) = 13.7 + 0.2 × degree of cerebellar ectopia (mm). $P < 0.001$

Patients with CM-1 have, on the average, a smaller, shallower PF than controls [7, 8, 10]. The fact that the difference was somewhat smaller in this study than in previous ones may be due to different selection criteria for patients and controls, different methods of PF size estimation, or to the fact that measurements in the present study were done in a strictly blinded way. A small, shallow PF thus seems to be associated with the CM-1 in a relatively large number of patients. Due to the considerable overlap between patients and controls, however, PF measurements can not be used as a diagnostic method for the CM-1.

Surprisingly, there were strong correlations between degree of cerebellar ectopia and the different measures of PF size (Table 5). To our knowledge, this has not been demonstrated previously; on the contrary, Schady et al. [8], in a study of 32 patients with CM-1, suggested a negative correlation. This suggestion was based on indirect evidence: of the 8 patients who had the most marked ectopia, 4 were among the 8 smallest as regards PF size. Vega et al. [7] found no significant correlation between degree of ectopia and the absolute PF volume. They did not, however, make correlations with the relative PF size. In addition, in both studies, the degree of cerebellar ectopia was only graded roughly, with reference to cervical vertebrae, and not measured in mm. Our data may therefore be the most reliable in this respect.

PF size: relation to pathogenesis

The prevailing hypothesis concerning the pathogenesis of the CM-1 is that it is due to a disproportion between PF which is originally too small and the growing hindbrain structures [6–8]. Several animal models exist for this condition [15–17]. In the studies by Marin-Padilla [16], high doses of vitamin A given to pregnant hamsters induced in the offspring, among other things, underdevelopment of the basiocciput and a small PF. This resulted in caudal displacement of the cerebellum which increased during its postnatal growth spurt. In humans, an abnormally small PF is usually considered part of a group of bony abnormalities of the base of the skull and the cervical spine termed occipital and suboccipital dysplasia. A disorder in three generations in a family has been described, with some family members having occipital dysplasia, some CM-1, and some both [6]. One mechanism for the development of a small PF may be a premature synostosis of the foramen magnum synchondroses, which has been observed in some infants [18]. A family with CM-1 without gross bony abnormalities has also been described [19].

In the light of these theories, the most likely interpretation of the positive correlation between the degree of ectopia and PF size is, in our opinion, that an originally too small PF has been moulded in the process of herniation of the hindbrain. When the growth spurt of the cerebellum occurs in a PF that is too small, the lowest part of the cerebellum (the tonsils) will be forced out through the for-

Table 6. Degree of cerebellar ectopia and PF ratio in different clinical presentations

	Degree of cerebellar ectopia (mm)		*P*	PF ratio (%)		*P*
Presentation	Absent	Present		Absent	Present	
Definite pathology[a]	8.6 ± 3.4 (n = 15)	14.3 ± 6.5 (n = 18)	0.005	15.4 ± 1.7 (n = 15)	16.3 ± 2.0 (n = 18)	0.2
Cerebellar symptoms or signs	9.2 ± 3.3 (n = 20)	15.5 ± 7.1 (n = 13)	0.002	15.3 ± 1.5 (n = 20)	16.9 ± 2.1 (n = 13)	0.02
Pyramidal signs	10.1 ± 4.3 (n = 28)	20.4 ± 7.1 (n = 5)	< 0.001	15.6 ± 1.8 (n = 28)	17.5 ± 1.9 (n = 5)	0.04
Syringomyelia	11.6 ± 6.7 (n = 25)	11.9 ± 2.9 (n = 8)	0.9	15.8 ± 2.0 (n = 25)	16.3 ± 1.8 (n = 8)	0.5
Headache	12.4 ± 5.2 (n = 19)	10.7 ± 6.9 (n = 14)	0.4	16.0 ± 2.0 (n = 19)	15.8 ± 1.8 (n = 14)	0.7

[a] Patients with syringomyelia on MRI or neurological signs probably due to the malformation

amen magnum, and at the same time the neural structures will tend to expand the PF, thus making its size more "normal". This theory may at least partly explain the overlap betwen patients with CM-1 and controls with regard to PF size, in this and previous studies [7, 8]. The large proportion of patients with CM-1 and a PF of normal size has puzzled investigators who think that a small PF may be the primary developmental defect in this condition [8].

Expansion of the PF occurs most easily prenatally or during the 1st year of life, before the closure of the sutures, but change of cranial proportions may occur until the age of 10 years at least [20]. Chronic tonsillar herniation has, however, been reported to occur even in adults after the placement of spinal subarachnoid shunts, where no herniation was present on gas myelography before shunting [21]. In such instances, it may be that the cerebellar tissue in fetal life was already deformed ("coned") by the process described above. This could make it herniate more easily later in life if a craniospinal pressure gradient is produced.

PF size: relation to clinical presentation

If this hypothesis concerning the pathogenesis of the malformation is correct, it would seem natural that some symptoms and signs may result from compression of tissues due to the disproportion between the hindbrain structures and the PF. Our observations indicate that the actual size of the PF is not a good indicator of the degree of disproportion since the PF may be passively moulded in the process of herniation at a relatively early stage. A better indicator of the disproportion would be the degree of ectopia. Compression of neural tissues may therefore be responsible for pyramidal signs and cerebellar symptoms and signs, because these were found to be associated with greater degrees of ectopia in both this and a previous study [22] (Table 6). In these subgroups of patients, the large PF ratio is probably only a passive reflection of a greater degree of herniation.

Another mechanism is probably responsible for the production of syringomyelia, since patients with this condition had approximately the same degree of ectopia and the same PF ratio as those without (Table 6). Current theories concerning the pathogenesis of syringomyelia associated with CM-1 emphasize the importance of altered CSF dynamics due to the valve action of the cerebellar tonsils in the foramen magnum [23] or to obstruction of the outflow foramina from the fourth ventricle [24]. These preconditions for the development of syringomyelia are probably at their maximum when herniation does not extend beyond a certain level. As in the present study, syringomyelia has previously been found to be associated with a moderate degree of ectopia [22]. It may, therefore, not be related to the degree of tissue compression due to the disproportion between neural and bony structures.

Headache was one of the most frequent complaints of patients with CM-1, and in different series it is reported to occur in 15–75% of patients [4, 5, 11, 22, 25–27]. The malformation may cause various kinds of headache with different pathogenetic mechanisms [28, 29]. Best understood is cough headache, probably due to the craniospinal pressure gradient generated by the valve action of the tonsils in the foramen magnum [30, 31]. This closely resembles one of the mechanisms that may be responsible for the production of syringomyelia. It seems, therefore, logical that patients with headache, just like as those with syringomyelia, did not on the average have particularly large herniations or PF ratios.

Conclusion

The present study indicates that the CM-1 in most patients, if not all, is due to an originally too small PF. There is, however, no evidence that a small PF by itself may be responsible for the production of symptoms and signs.

In future morphometric studies of the CM-1 the most fruitful approach may be to correlate different clinical presentations with precise measurements of the neural malformations as seen with MRI. The intimate relationship, however, between the malformed neural structures and an abnormal bony encasement in the pathogenesis of the malformation should always be taken into consideration.

References

1. Chiari H (1891) Über Veränderungen des Kleinhirns infolge von Hydrocephalie des Grosshirns. Dtsch Med Wochenschr 17: 1172–1175

2. Chiari H (1896) Über Veränderungen des Kleinhirns, des Pons und Medulla oblongata infolge von congenitaler Hydrocephalie des Grosshirns. Dtsch Med Wochenschr 63: 71–116
3. Spillane JD, Pallis C, Jones AM (1957) Developmental abnormalities in the region of the foramen magnum. Brain 80: 11–48
4. Mohr PD, Strang FA, Sambrook MA, Boddie HG (1977) The clinical and surgical features in 40 patients with primary cerebellar ektopia (adult Chiari malformation). Q J Med 46: 85–96
5. Dysthe GN, Menezes AH, Van Gilder JC (1989) Symptomatic Chiari malformations. J Neurosurg 71: 159–168
6. Coria F, Quintana F, Rebollo M, Combarros O, Berciano J (1983) Occipital dysplasia and Chiari type I deformity in a family. J Neurol Sci 62: 147–158
7. Vega A, Quintana F, Berciano J (1990) Basichondrocranium anomalies in adult Chiari type I malformation: a morphometric study. J Neurol Sci 99: 137–145
8. Schady W, Metcalfe RA, Butler P (1987) The incidence of craniocervical bony anomalies in the Chiari malformation. J Neurol Sci 82: 193–201
9. Krogness KG (1978) Posterior fossa measurements. I. The normal size of the posterior fossa. Pediatr Radiol 6: 193–197
10. Nyland H, Krogness KG (1978) Size of posterior fossa in Chiari type I malformation. Acta Neurochir (Wien) 40: 233–242
11. Levy WJ, Mason L, Hahn JF (1983) Chiari malformation presenting in adults: a surgical experience with 127 cases. Neurosurgery 12: 377–390
12. Aboulezz AO, Sartor K, Geyer CA, Gado MH (1985) Position of cerebellar tonsils in the normal population and in patients with the Chiari malformation: a quantitative approach with MR imaging. J Comput Assist Tomogr 9: 1033–1036
13. Barkovich AJ, Wippold FJ, Sherman JL, Citrin CM (1986) Significance of cerebellar tonsillar position. AJNR 7: 795–799
14. Woolson RF (1987) Statistical methods for the analysis of biomedical data. Wiley, New York, pp 59–64
15. Margolis G, Kilham L (1969) Experimental virus-induced hydrocephalus. Relation to pathogenesis of the Arnold-Chiari malformation. J Neurosurg 31: 1–9
16. Marin-Padilla M, Marin-Padilla TM (1981) Morphogenesis of experimentally induced Arnold-Chiari malformation. J Neurol Sci 50: 29–55
17. Hung CF, Nakagata N, Sato K (1989) The morphogenesis of hindbrain crowding associated with lumbosacral myeloschisis. Neurol Med Chir 29: 981–988
18. Kruyff E (1965) Occipital dysplasia in infancy. The early recognition of craniovertebral abnormalities. Radiology 85: 501–507
19. Stovner LJ, Cappelen J, Nilsen G, Sjaastad O (1992) The Chiari type I malformation in two MZ twins and first degree relatives. Ann Neurol 31: 220–222
20. Jacobson RI (1985) Abnormalities of the skull in children. Neurol Clin 3: 117–145
21. Welch K, Shillito J, Strand R (1981) Chiari I "malformation": an acquired disorder? J Neurosurg 55: 604–609
22. Pillay PK, Awad IA, Little JD, Hahn JF (1991) Symptomatic Chiari malformation in adults: a new classification based on magnetic resonance imaging with clinical and prognostic significance. Neurosurgery 28: 639–645
23. Williams B (1986) Progress in syringomyelia. Neurol Res 8: 130–145
24. Gardner WJ (1965) Hydrodynamic mechanism of syringomyelia: its relationship to myelomeningocele. J Neurol Neurosurg Psychiatry 28: 247–259
25. De Barros MC, Farias W, Ataide L, Lins S (1968) Basilar impression and Arnold Chiari malformation. A study of 66 cases. J Neurol Neurosurg Psychiatry 31: 596–605
26. Saez RJ, Onofrio BM, Yanagihara T (1976) Experience with the Arnold-Chiari malformation, 1960–1970. J Neurosurg 45: 416–422
27. Paul KS, Lye RH, Strang FA, Dutton J (1983) Arnold-Chiari malformation. Review of 71 cases. J Neurosurg 58: 183–187
28. Khurana RK (1991) Headache spectrum in Arnold-Chiari malformation. Headache 31: 151–155
29. Thomas M, Boyle R (1979) A possible connection between basilar migraine and the Arnold-Chiari malformation. Neurology 29: 527–528
30. Williams B (1981) Simultaneous cerebral and spinal fluid recordings. 2. Cerebrospinal dissociation with lesion at the foramen magnum. Acta Neurochir (Wien) 59: 123–142
31. Williams B (1980) Cough headache due to craniospinal pressure dissociation. Arch Neurol 37: 226–230

Dr. L. J. Stovner
Department of Neurology
Trondheim University Hospital
N-7006 Trondheim
Norway